Targeting Angiogenesis for Mammary Cancer Prevention: Factors to Consider in Experimental Design and Analysis

Henry J. Thompson, John N. McGinley, Pamela Wolfe, Nicole S. Spoelstra, and Katrina K. Knott

Cancer Prevention Laboratory, Colorado State University, Fort Collins, Colorado

Abstract

An experimental model developed to investigate premalignant stages of breast cancer was used to establish a rationale for designing experiments that target angiogenesis for cancer prevention. Blood vessels were identified via CD31 immunostaining, and all vessels that occurred in a 50 μm wide region circumscribing each pathology were counted using a digital imaging technique. The blood vessel density associated with terminal end buds was unaffected by carcinogen treatment, whereas vessel density was higher in intraductal proliferations and ductal carcinoma in situ than in terminal end buds ($P < 0.001$) and total vascularity increased with morphologic progression. In comparison with intraductal proliferation or ductal carcinoma in situ, mammary carcinomas had higher vascular density in the tissue surrounding the cancer with a marked increase in the number of blood vessels <25 μm^2. These data suggest that antiangiogenic chemopreventive agents would inhibit cancer occurrence if initiated at any premalignant stage of the carcinogenic process. Because increased vascular density observed during premalignancy could be explained by the size expansion of the lesion and its encroachment on a preexisting blood supply, by pathology-associated vessel expansion, and/or by angiogenesis, it remains to be determined if antiangiogenic agents will reduce the prevalence of premalignant lesions or cause their accumulation by blocking conversion to carcinomas. Failure to recognize the patterns of vascularization that accompany morphologic progression could limit the success of efforts to target angiogenesis for cancer prevention and lead to misinformation about how agents that affect blood vessel formation or growth inhibit the carcinogenic process. (Cancer Epidemiol Biomarkers Prev 2004;13(7):1173–84)

Introduction

There is an emerging awareness that cancer preventive agents are likely to work by multiple mechanisms (1). One candidate mechanism that is receiving an increasing amount of attention is angiogenesis (2, 3), the process of neovascularization that has been reported to provide blood to support not only newly forming tissues but also malignant pathologies (4). However, investigation of the role of angiogenesis in early stages of the progression of premalignant pathologies to cancer has received limited attention. In this article, we report on the pattern of change in vascular density during the morphologic progression of premalignant breast disease as a model for future investigations of angiogenesis and cancer prevention.

Investigations of the role of angiogenesis in premalignant breast disease are limited in number, the methods used to assess vascularity have varied, and, not surprisingly, different findings have been reported (5-11). Among those differences particularly relevant to chemoprevention are (1) whether an increase in vascularity is induced during premalignant breast disease and (2), if vascularity is increased, whether it is due to an increase in the area and/or the number of blood vessels per unit of assessed area. Moreover, comparisons of the degree of angiogenesis observed in either premalignant or malignant breast disease with the magnitude of angiogenesis observed in morphologically identifiable normal mammary gland structures during different developmental states of the mammary gland have not been published. Such comparisons would permit an assessment of whether the process of neoplastic transformation in the breast involves an increase in the angiogenic potential of the involved epithelium in comparison with the induction of angiogenesis observed under physiologic conditions and potentially could serve as a positive control for use in data interpretation.

Chemically induced rat models for breast cancer are widely used to investigate the genesis and prevention of this disease (12). In the rat, the terminal end bud (TEB) is considered the morphologic structure that is the putative target of insult and transformation induced by chemical carcinogens; in humans, the terminal ductal lobular unit is considered the comparable target structure (13-15). Cells within TEBs are observed to progress to cancer in steps parallel to those observed in the human disease and include mild, moderate, and florid hyperplasia of the usual type [hyperplasias are called intraductal proliferations (IDP) in the rat], ductal carcinoma *in situ* (DCIS), and invasive adenocarcinomas (AC; refs. 12, 16).

Received 10/6/03; revised 2/20/04; accepted 2/25/04.

Grant support: USPHS grant CA52626 from the National Cancer Institute.

The costs of publication of this article were defrayed in part by the payment of page charges. This article must therefore be hereby marked advertisement in accordance with 18 U.S.C. Section 1734 solely to indicate this fact.

Requests for reprints: Henry J. Thompson, Cancer Prevention Laboratory, Colorado State University, 111 Shepardson Building, 1173 Campus Delivery, Fort Collins, CO 80523-1173. Phone: 970-491-7748; Fax: 970-491-1004.
E-mail: henry.thompson@colostate.edu

Differences in these disease processes include that human breast carcinomas generally have greater cellular heterogeneity and a more extensive stromal component than mammary carcinomas induced in the rat and that rat mammary carcinomas metastasize infrequently.

Almost 25 years ago, angiogenesis was reported to be induced in the mammary gland following treatment of female rats with chemical carcinogens (17, 18), but only a limited amount of work has been done in the intervening years to pursue those initial observations (19). Nonetheless, that early work and other studies using explants of premalignant rodent (20, 21) or human (5, 22-24) breast tissue in the rabbit iris angiogenesis assay suggest that rodent models for breast cancer are appropriate for the investigation of angiogenesis.

Our laboratory has modified the protocol of carcinogen administration as proposed by Gullino et al. (25) to facilitate the investigation of both premalignant and malignant stages of mammary carcinogenesis (26). Using that model and a method recently published by our laboratory to quantify vascular density (27), experiments were conducted to address the following questions: (1) Can carcinogen treatment associated changes in the vascular density of TEBs be used to assess the effects of cancer preventive agents on angiogenesis? (2) Does vascular density increase during morphologic progression of premalignant pathologies and, if it does, is it due to an increase in vessel number and/or size? and (3) How does vascularization of premalignant mammary gland pathologies compare with that observed in mammary carcinomas or in the mammary gland during pregnancy? In our judgment, answers to these questions will facilitate the design and interpretation of cancer prevention studies in which the candidate mechanism being investigated is angiogenesis.

Materials and Methods

Chemicals and Reagents. The carcinogen, 1-methyl-1-nitrosourea (MNU), was obtained from Ash Stevens (Detroit, MI). Donkey serum (Jackson ImmunoResearch Laboratories, West Grove, PA) was used as blocking serum to prevent nonspecific binding of primary antibodies. Goat anti-CD31 antibody was obtained from Research Diagnostics (Flanders, NJ). Horseradish peroxidase–conjugated streptavidin (DAKO Corp., Carpinteria, CA) and stable 3,3′-diaminobenzidine (Research Genetics, Huntsville, AL) were used in the visualization of blood vessels.

Animals. Female Sprague-Dawley rats were obtained from Taconic Farms (Germantown, NY) at 20 days of age. Rats were injected with 50 mg MNU per 1 kg body weight at 21 days of age, and the experiment was terminated 35 days postcarcinogen as described previously (26). At necropsy, whole mounts of abdominal inguinal mammary gland chains (glands 4 to 6) were prepared, and tissue was fixed in formalin. The fixed tissue was stained, and stained whole mounts were photographed and evaluated under 2× magnification for detection of any abnormality that might be a mammary pathology. All abnormalities were excised from whole mounts and processed for histologic classification as described previously (28). Premalignant pathologies were randomly selected from the abdominal inguinal mammary glands and further evaluated for vascular density. The following pathologies were evaluated: IDP with mild, moderate, or florid hyperplasia, DCIS, and AC. Two positive controls were evaluated. They were TEBs excised from carcinogen- and non-carcinogen–treated rats and lobules from midpregnant mammary gland (MPMG).

Assessment of Vascular Density. The method for immunostaining of mammary tissue for blood vessel detection has been reported in detail (27). Briefly, paraffin sections from formalin-fixed mammary tissue and mammary pathologies were cut at 4 μm and mounted onto 3-aminopropyltriethoxysilane–treated slides. Sections were processed for immunostaining of blood vessels using antiserum directed against the CD31 epitope. Census counting of all blood vessels was undertaken. In assessing TEB, IDP, and DCIS, blood vessels were not found within these morphologic structures; therefore, blood vessel density was quantified in a 50 μm wide band of mammary tissue circumscribing each structure. For MPMG, vessel density was measured within lobules and in a 50 μm wide band of tissue circumscribing each lobule. For mammary carcinomas, vascular density was determined both within the tumor and in a 50 μm wide band of mammary tissue circumscribing each carcinoma. Based on empirical evidence, a 50 μm wide region was selected because it could be uniformly applied without spatial overlap to both normal structures within the mammary gland such as TEBs and premalignant and malignant mammary gland pathologies. Moreover, this region included the area of most intense pathology-associated angiogenic activity irrespective of the histologic classification of the pathology.

Vessels were counted using images of immunostained sections captured with a Kodak DCS-420 digital camera (Eastman Kodak, Rochester, NY) mounted on a Zeiss Axioskop microscope using a 10× objective. The photographic coupler has a 10× ocular, and the CCD imaging sensor on the DCS-420 has a focal magnification of 2.5× yielding images with an approximate total magnification of 250×. The resolution of each image was 1,012 × 1,524 or 1.5 MP. Images were acquired using a 32-bit Kodak TWAIN driver version 5.02 within Adobe Photoshop version 4.0 graphic software (Adobe Systems, Inc., San Jose, CA) running on a 300 MHz Pentium III PC with 128 MB RAM. Lesions that exceeded the size of a single imaging area were captured by photographing contiguous microscopic fields in a raster pattern. Each captured image was merged using a layer technique in Adobe Photoshop to form a single composite image for analysis. All vessels were circumscribed manually using a digitizing pen to rule out inclusion of artifact or background immunostain. Criteria established by Weidner and Folkman (29) were used to identify blood vessels in immunostained sections. Specifically, positively stained endothelial cells or endothelial cell clusters, regardless of size or shape, which were clearly separate from adjacent blood vessels, mammary epithelial cells, or other connective tissue elements, were counted. Vessel lumens, although usually present, were not necessary for a structure to be defined as a blood vessel, and RBCs were not used to define a vessel lumen. As outlined in ref. 30, vessels were assigned to one of five categories based on size.

The number of animals, the number of normal structures and pathologies of each type, and the number of blood vessels of each size counted in each normal structure or type of pathology are summarized in Table 1.

Statistical Methods

Blood Vessel Counts. The primary consideration in statistical analyses of the vascular density count data was the presence of zero values, because many of the microscopic fields examined using the census counting technique contained no blood vessels of a particular size category (zero counts). The usual distribution assumed for count data is either the Poisson or the negative binomial; the negative binomial distribution differs from the Poisson in its specification of the variance. Either model will underpredict in the left tail of the distribution when an excess of zeros is present. Zero inflated models introduce an additional component to the distribution function to account for observations that will always have zero counts; final estimates are based on a combination of the probability of observing a particular count with the probability of being in the ''always zero'' category. For these reasons, a zero inflated negative binomial model was used as a component of the analysis plan for evaluating blood vessel count data (31).

Blood Vessel Area. While the blood vessel area data were approximately log normal and the log-transformed data were distributed as approximately normal, they were truncated at zero due to the presence of areas without vascularization in particular vessel size classes. Tobit estimation was originally developed in the context of consumer demand, where preferences are measured by the dollar amount spent, and data are typically censored at zero. The Tobit method has been adapted to handle left censored data, right censored data, or both and is the method of choice for modeling truncated normal data. Consequently, a Tobit model was used as a component of the statistical analysis plan for blood vessel area data (32).

Tests of Central Tendency. The advantage of the parametric models described is that, when the distributional assumptions hold, they are generally more powerful than nonparametric methods, and adjustment for covariates can be readily incorporated. Most of the comparisons of interest resulted from straightforward questions about relative vascular density between two or more conditions and did not require modeling as such. For questions involving the differences in central tendency for blood vessel count or area between two or more conditions or trend across conditions, nonparametric tests are more robust than parametric tests when the distributional assumptions do not hold. Two-sample and k-sample rank tests and median tests are simply functions of the rank scores of the values of the response variables or the number of observations in a group falling below the median of the entire sample; no other transformation is required; groups are assumed to be independent. A more general nonparametric approach that relies only on the empirical distribution for determining P values is the bootstrap, resampling with replacement from the observed data under the assumption that the null hypothesis is true (33). Wilcoxon tests, median tests, and bootstrap P values were computed for both count and area data (34). Trends in central tendency across conditions were evaluated by the Jonckheere-Terpstra test for ordered alternatives (34). This test can be used when the alternative hypothesis is stated $\tau_1 \leq \tau_2 \leq \ldots \leq \tau_k$ and at least one strict inequality holds; τ_i is the median of the ith group.

Other Considerations. Because five vessel size categories were evaluated for each morphologic structure, measurements within morphologic structure were not independent (i.e., measurements within a given structure were more alike than measurements between morphologic structures of the same type). This is called a clustering effect, and clustering influences the estimates of standard errors; this clustering effect was accounted for in both the zero inflated negative binomial model and the Tobit model. Results were comparable across statistical methods, suggesting that the parametric models are appropriate for these data and that the nonparametric methods provide reliable results for exploration; all P values

Table 1. Summary of the number of animals, tissues, and blood vessels that were evaluated

MNU	DPC	Days of Age	No. of Animals	Structures	No. of Structures	Location	No. of Blood Vessels by Vessel Size Category (μm^2)				
							≤10	>10 and ≤25	>25 and ≤50	>50 and ≤75	>75
No	0	21	7	TEB	108	P	0	10	72	49	60
No	0	49	12	TEB	36	P	15	61	21	13	18
No	0	56	19	TEB	81	P	12	95	35	5	12
Yes	28	49	12	TEB	40	P	16	58	38	9	28
Yes	35	56	20	TEB	84	P	50	86	24	10	38
Yes	35	56	9	IDP, MILD	9	P	0	46	80	26	52
Yes	35	56	8	IDP, MOD	11	P	4	56	113	57	105
Yes	35	56	9	IDP, FLORID	10	P	2	94	194	111	271
Yes	35	56	7	DCIS	9	P	4	50	83	54	152
Yes	35	56	18	AC	18	ET	263	750	375	158	494
Yes	35	56	18	AC	18	IT	74	201	78	26	44
No	0	73	8	MPMG	8	EL	28	149	44	7	10
No	0	73	8	MPMG	8	IL	131	320	43	14	27

NOTE: DPC, days post carcinogen. Location: P, peripheral to the structure or pathology (a 50 μm wide band circumscribing each structure); ET, extratumoral; IT, intratumoral; IL, intralobular; and EL, extralobular. Structures: IDP MILD, IDP with mild hyperplasia; IDP MOD, IDP with moderate hyperplasia; and IDP FLORID, IDP with florid hyperplasia.

reported were based on bootstrap results unless stated otherwise. All Tobit and zero inflated binomial analyses were done in STATA version 7.0. Exploratory assessment, graphs, and nonparametric analyses were done in SAS version 8.1 and SYSTAT version 10.

Results

The staining of blood vessels in mammary tissue with CD31 was crisp with limited background staining and no distortion of tissue architecture. Figures 1 and 2 include photomicrographs of a TEB and of premalignant pathologies showing a representative example of each type of lesion assessed. Note that, in all cases, vascularization was limited to the area outside the lesion (i.e., in no case had blood vessels penetrated the basement membrane of the mammary pathology). This is unlike the pattern of vascularization observed in mammary carcinomas (as illustrated in Fig. 3) in which blood vessels were observed not only in the 50 μm wide band surrounding a tumor but also within the tumor mass. Figure 3 also shows the pattern of vascularization observed in the MPMG.

Can Vascular Density of TEBs Be Used to Assess the Effects of Cancer Preventive Agents on Angiogenesis? TEBs were evaluated from non-carcinogen–treated animals euthanized on the day carcinogen was administered (21 days of age) and from both carcinogen- and non-carcinogen–treated animals at 28 (49 days of age) and 35 (56 days of age) days postcarcinogen, times at which premalignant and malignant pathologies are known to exist in the mammary glands of rats in this model system (35). Data in Table 2 give a detailed compilation of vascular density (expressed as blood vessel count or area per unit of assessed area) using five previously published vessel size criteria (30).

The most striking feature of data in Table 2 was the lack of blood vessels in the various size categories that were assessed. Statistical analyses were performed on these data to determine if either vessel counts or vessel area (total or by vessel size category) were affected by treatment with MNU, controlling for potential contributions of age of the animal. Using the zero inflated negative binomial and Tobit models, no evidence was obtained that carcinogen treatment had an affect on vascular density of TEB measured as counts ($P = 0.10$) or area ($P = 0.12$) per unit of area assessed, and the effect of age on vascular density in either statistical model was not significant. Bootstrap results for the effects of MNU were less significant in the count data ($P = 0.54$) and no different in the area data ($P = 0.13$). The nonparametric tests for differences by age and the Jonckheere-Terpstra trend test for area data gave results comparable with the parametric models. In the count data, density increased significantly (bootstrap estimates) from 21 to 49 days of age ($P = 0.0007$) but not from 49 to 56 days of age ($P = 0.6$).

The analysis of the TEB data was extended to address the question of whether there were populations of TEB in carcinogen-treated animals that differed in vascularity

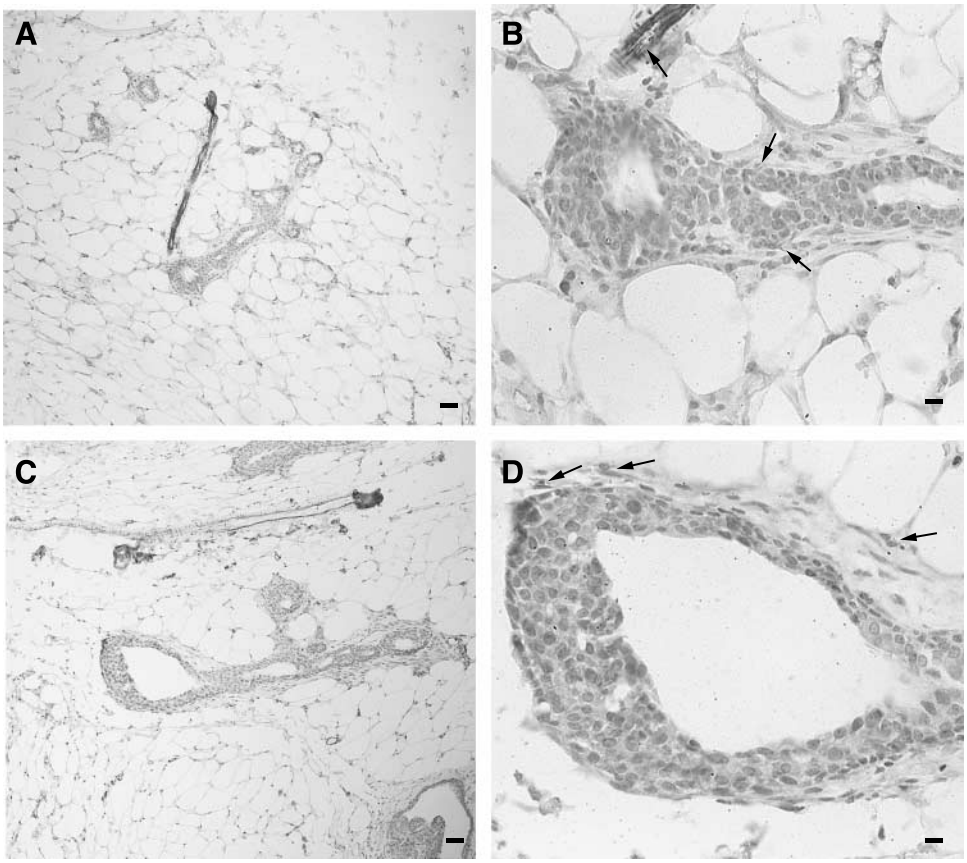

Figure 1. A. Low magnification (×100) control TEB. **B.** High magnification (×400) control TEB. Note normal ductal epithelium of one to two cell layers thick. Small blood vessels are apparent in the thicker collagen band area at the proximal end of the TEB, enabling unobstructed extension of the distal end into the fat pad. *Arrows,* blood vessels. A large blood vessel is located near the distal end of the TEB. **C.** Low magnification (×100) mild IDP. **D.** High magnification (×400) mild IDP. Note multiple cell layers and a patent lumen. Blood vessels appear in a pattern similar to TEB. However, more collagen is present in the distal portion of the lesion, and blood vessels begin to extend around the IDP. Blood vessels are limited to mammary tissue circumscribing each structure as indicated by *arrows*. **A** and **C.** Bars = 50 μm. **B** and **D.** Bars = 10 μm.

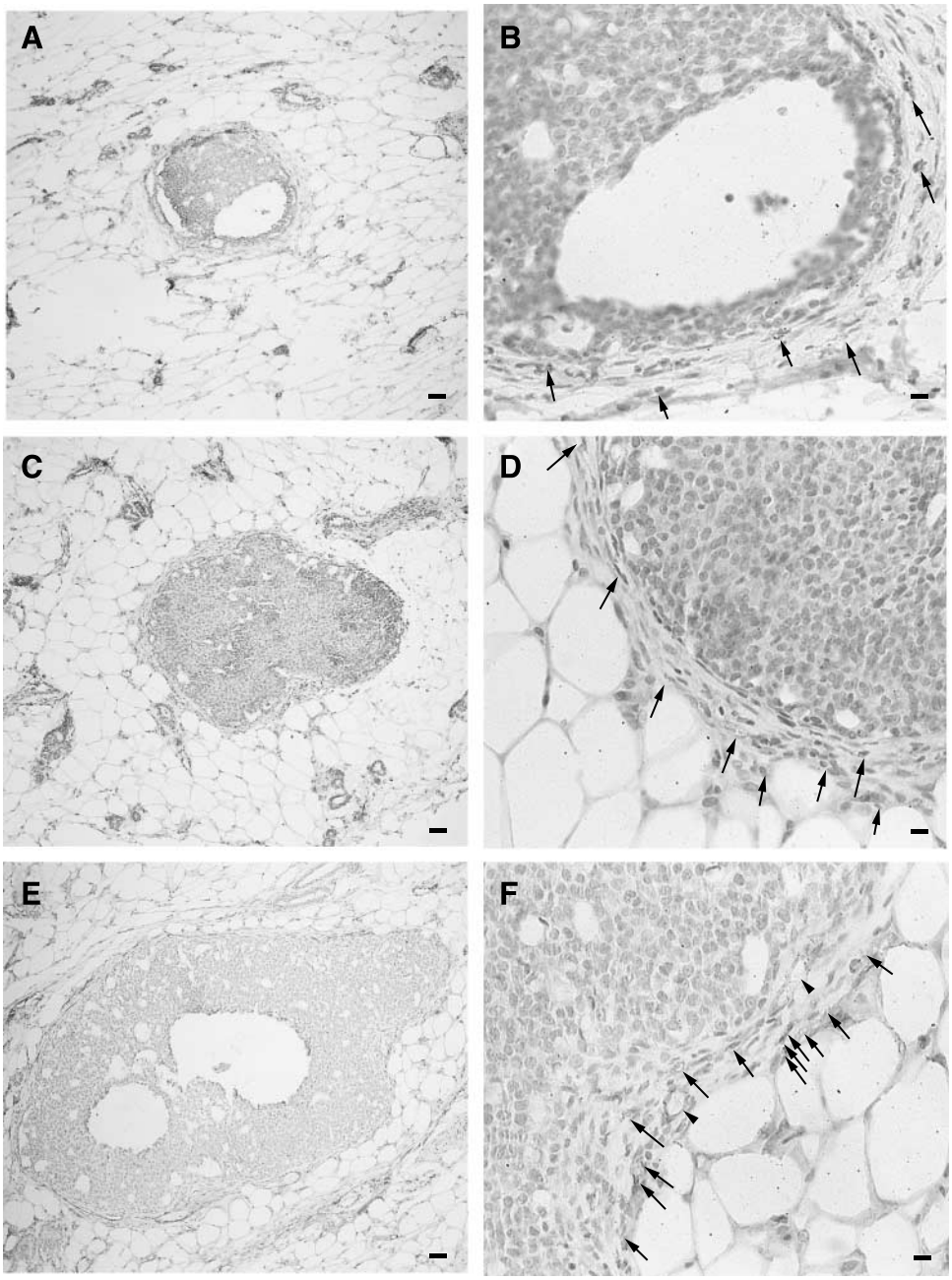

Figure 2. **A.** Low magnification (×100) moderate IDP. **B.** High magnification (×400) moderate IDP. Note increased cell layers, smaller primary lumen, and presence of irregular secondary lumina. Blood vessels are limited to mammary tissue circumscribing each structure as indicated by *arrows*. **C.** Low magnification (×100) florid IDP. **D.** High magnification (×400) florid IDP. Nuclei are hyperchromatic. Note that primary lumen is occluded and the numerous irregular secondary lumina. Blood vessels are limited to mammary tissue circumscribing each structure as indicated by *arrows*. **E.** Low magnification (×100) DCIS. **F.** High magnification (×400) DCIS. Nuclei are slightly larger and more rounded and exhibit moderate homogenous chromasia. Cribriform spaces are apparent. Blood vessels are limited to mammary tissue circumscribing each structure as indicated by *arrows*. **A**, **C**, and **E.** Bars = 50 μm. **B**, **D**, and **F.** Bars = 10 μm.

and that might identify TEBs that were likely to undergo morphologic progression. The rationale for this analysis was that a subset of TEBs might exist with higher levels of vascularization, an effect that could be obscured from detection in the statistical analyses reported in the preceding paragraph. To evaluate this possibility, data in Table 2 were further evaluated using a nonparametric clustering algorithm. Neither the count data nor the area data exhibited statistically significant clusters of TEBs that differed by vascularity.

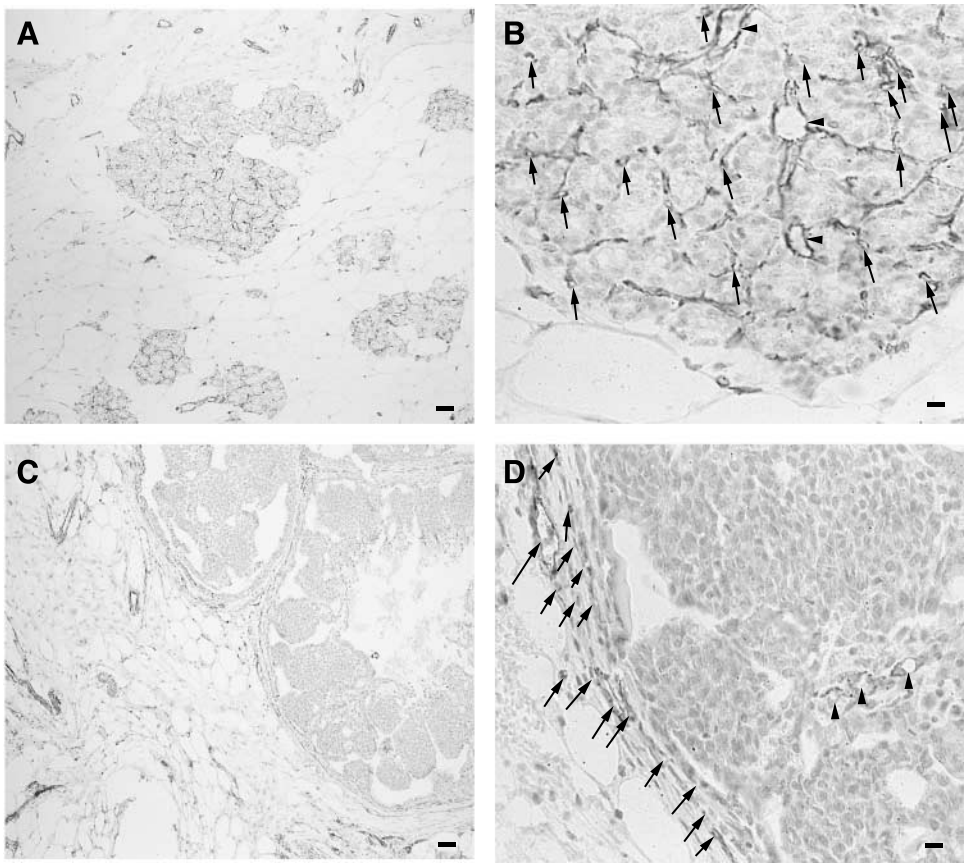

Figure 3. A. Low magnification (×100) lobule from control pregnant mammary gland. **B.** High magnification (×400) lobule from control pregnant mammary gland. *Arrowheads,* large intralobular blood vessels. *Arrows,* cross-sections of small intralobular vessels. Numerous longitudinal blood vessels are visible within the intralobular spaces. **C.** Low magnification (×100) AC. **D.** High magnification (×400) AC. Blood vessels within the tumor (*arrowheads*) indicate that the basement membrane has been breached; these vessels are thus called intratumoral blood vessels. *Arrows,* extratumoral vessels.

Does Vascular Density Increase during Morphologic Progression of Premalignant Pathologies? As a first step in addressing this question, total vascular density measured as blood vessel counts or area was assessed to determine if the vascularity of TEBs was different from that of IDP and DCIS (Fig. 4A and B). For this analysis, only TEBs from 56-day-old MNU-treated animals were included to maintain age comparability. The same pattern of vascularization was observed when vascular density data were expressed as blood vessel counts or blood vessel area per unit of assessed area. Vascular density was significantly higher in IDP or DCIS relative to TEBs ($P < 0.0001$) for both area and count data. Further analyses of these data indicated that this effect could be attributed primarily to the number and area of blood vessels in size categories ≥3 (i.e., blood vessels ≥ 25 μm^2 in cross-sectional area; $P < 0.01$).

The second question addressed was ''Does vascularity increase with the morphologic progression of premalignant pathologies?'' For this analysis, TEBs were not included in the modeling because their inclusion forced most trend estimates to be significant, blurring the relationship among IDP of various types and DCIS. Total vascular density increased with morphologic progression (mild IDP → moderate IDP → florid IDP → DCIS). This trend in total vascularity was significant for total counts ($P = 0.03$) and total area ($P = 0.003$) based on the Jonckheere-Terpstra test for ordered alternatives. The same trend was also observed when vessel density was analyzed using parametric models; however, these analyses indicated that the trend was due primarily to blood vessels in size category 5 ($P < 0.001$).

How Does Vascularization of Premalignant Mammary Gland Pathologies Compare with That Observed in Mammary Carcinomas or in the Mammary Gland During Pregnancy? Table 3 shows the vascular density for mammary carcinomas and MPMG. Total vascular density count or area was higher in AC than in IDP ($P < 0.001$; Fig 4). Vascular density also was higher in mammary carcinomas than in DCIS for count data ($P = 0.01$) but not area data ($P = 0.14$). The difference in vascular density between AC and either IDP or DCIS was primarily due to an increase in blood vessels >25 μm^2 in cross-sectional area (size categories 1 and 2). In addition, blood vessels were observed both within (intratumoral) and around (extratumoral) the periphery of the mammary carcinomas, unlike the pattern of vascularization observed in IDP or DCIS.

Vascular density of the MPMG was operationally divided into two zones that have parallels to the zones evaluated in mammary carcinomas. The peripheral zone represents the area that was within a 50 μm wide band that circumscribed each mammary gland lobule; this zone was comparable with the extratumoral region of mammary carcinomas. The intralobular region represented the vasculature lying immediately adjacent to the mammary epithelium comprising the developing lobules of the MPMG and compared with the intratumoral region of carcinomas in which blood vessels lie adjacent to the developing neoplastic epithelial cells. Data in Table 3 show the vascular profile of the peripheral and intralobular regions of the MPMG. Comparing AC with MPMG in the peripheral region, the MPMG was dominated by vessels in size classes 1 ($P < 0.02$) and 2 ($P < 0.09$), whereas there was a greater preponderance of blood vessels in size categories 4 ($P < 0.0001$) and 5 ($P < 0.0001$) in mammary carcinomas. Total vascular density in the peripheral zone based on count data was greater in MPMG than AC ($P < 0.0001$), while, based on total area, AC was more vascular than MPMG but not significantly so ($P = 0.18$). When vascular data from the intratumoral and intralobular regions were evaluated, vascular density was greater (both area and count) in MPMG ($P < 0.0001$). When vascular data from all sources and vessel size classes were combined (Table 3, last column), vascularity count data were greater in MPMG than AC; however, the difference between AC and midpregnant mammary tissue was not statistically significant. Overall, the differential response noted in vessel count versus vessel area data between AC and MPMG was due to relative differences in the distribution of blood vessel size: size classes 1 to 3 predominated in the MPMG, whereas size classes 4 and 5 predominated in AC.

Discussion

Current understanding about the role of angiogenesis in mammary carcinogenesis is limited, and the information that exists is contradictory. Consequently, we do not know what stage (if any) of premalignant disease progression is dependent on new vessel formation (10, 36). In view of this, it is of interest that data have recently been published reporting proof-in-principle that inhibition of angiogenesis early in mammary carcinogenesis prevents mammary tumor formation (36). While that report is consistent with other work indicating that angiogenesis is a potential target for cancer chemoprevention (1-3), it has yet to be shown *in vivo* that inhibition of blood vessel formation during premalignant stages of the disease process is associated with disease prevention. We judge that there are several reasons for the dearth of available information and its contradictory nature and that an *in vivo* assay different than those currently employed to study tumor angiogenesis is needed to resolve these issues. We also argue that such an approach will complement others that have been used to study the effects of cancer preventive agents on angiogenesis. Among those approaches are (1) the use of xenografts (37), (2) the isolation of cells from a tissue and

Table 2. Vascular density of TEBs as categorized by blood vessel size

n	MNU	DPC	Type	Vessel size classification scheme (μm^2)					
				≤10	>10 and ≤25	>25 and ≤50	>50 and ≤75	>75	Total
93	No	0	Count*,†	0.0 (0.0, 0.0)	0.0 (0.0, 0.0)	27.5 (0.0, 38.0)	0.0 (0.0, 31.5)	0.0 (0.0, 35.4)	56.5 (37.6, 91.1)
			Area*,‡,§	0.0 (0.0, 0.0)	0.0 (0.0, 0.0)	968.9 (0.0, 1,375.3)	0.0 (0.0, 1,953.7)	0.0 (0.0, 5,600.5)	3,988.2 (2,015.8, 6,838.8)
34	No	28	Count	0.0 (0.0, 0.0)	40.0 (0.0, 92.9)	0.0 (0.0, 35.0)	0.0 (0.0, 27.3)	0.0 (0.0, 34.6)	94.2 (62.7, 146.9)
			Area	0.0 (0.0, 0.0)	700.9 (0.0, 1,188.0)	0.0 (0.0, 985.0)	0.0 (0.0, 1,715.0)	0.0 (0.0, 5,177.4)	2,635.2 (1,857.3, 9,676.9)
40	Yes	28	Count	0.0 (0.0, 13.3)	24.2 (0.0, 45.3)	13.2 (0.0, 37.4)	0.0 (0.0, 0.0)	0.0 (0.0, 23.4)	71.3 (45.5, 93.5)
			Area	0.0 (0.0, 84.0)	378.8 (0.0, 675.9)	405.4 (0.0, 1,208.7)	0.0 (0.0, 0.0)	0.0 (0.0, 6,005.2)	1,763.9 (784.4, 8,596.8)
75	No	35	Count	0.0 (0.0, 0.0)	48.5 (29.8, 74.0)	0.0 (0.0, 36.4)	0.0 (0.0, 0.0)	0.0 (0.0, 0.0)	73.9 (50.3, 101.3)
			Area	0.0 (0.0, 0.0)	785.8 (380.0, 1,209.0)	0.0 (0.0, 1,206.5)	0.0 (0.0, 0.0)	0.0 (0.0, 0.0)	1,744.6 (1,100.8, 2,843.1)
70	Yes	35	Count	0.0 (0.0, 28.2)	32.1 (0.0, 61.2)	0.0 (0.0, 0.0)	0.0 (0.0, 0.0)	0.0 (0.0, 29.0)	72.2 (144.4, 114.6)
			Area	0.0 (0.0, 222.9)	453.1 (0.0, 903.8)	0.0 (0.0, 0.0)	0.0 (0.0, 0.0)	0.0 (0.0, 7,886.4)	3,035.2 (1,199.0, 8,920.2)

NOTE: DPC, days post carcinogen.
*All values are expressed as medians (upper limit, lower limit of the interquartile range: the lower limit is the 25th percentile and the upper limit is the 75th percentile). Fifty percent of the data lie in the interquartile range, which is a stable measure of dispersion for small samples. A tabular presentation in which these data are expressed as means ± SEM or medians with 95% confidence intervals can be accessed at http://cpl.colostate.edu/angiogenesis.
†Count data are number of blood vessels per unit of assessed area (mm^2) within the indicated vessel size criteria.
‡Area data are blood vessel area (μm^2) per unit of assessed area (mm^2) within the indicated vessel size criteria.
§Statistical evaluation of these median data as described in Materials and Methods indicated that carcinogen treatment did not increase vascular density of TEBs measured as area ($P = 0.13$) or counts ($P = 0.54$) per unit of area assessed. Similar nonsignificant results were obtained with the zero inflated negative binomial analysis of the count data and the Tobit analysis of the area data.

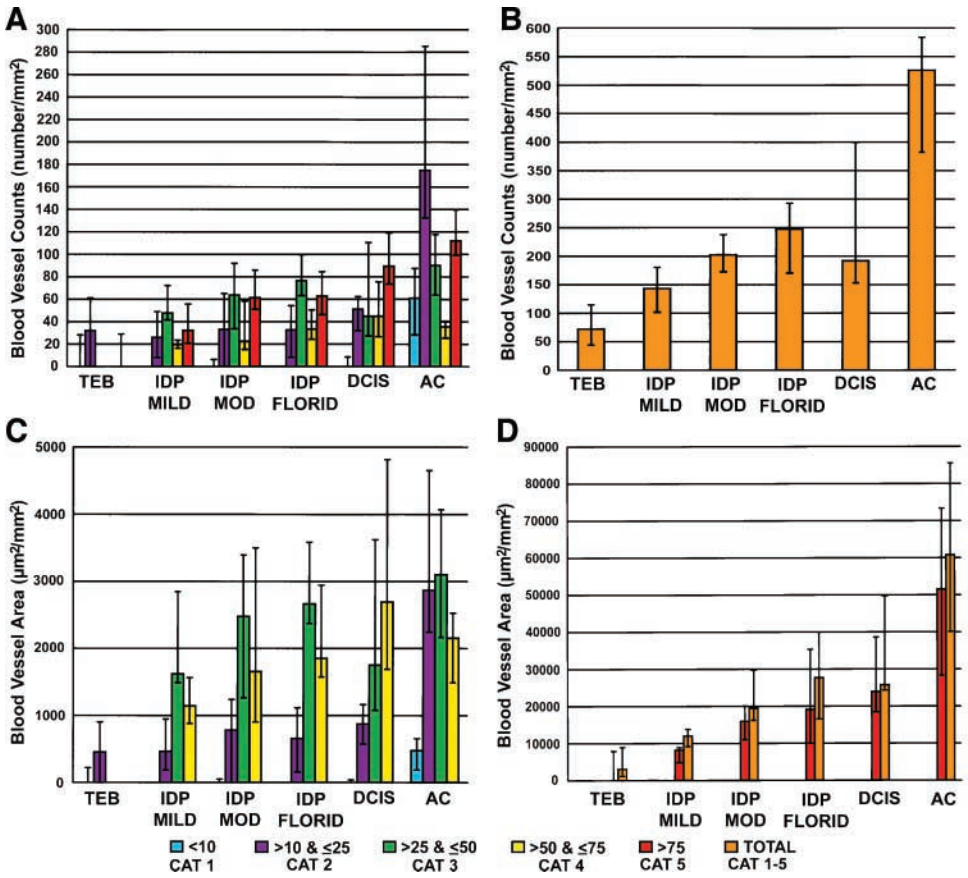

Figure 4. Blood vessel counts or blood vessel area per unit of assessed area for TEB, IDP with mild (*IDP MILD*), moderate (*IDP MOD*), or florid hyperplasia (*IDP FLORID*), and AC. Data are plotted for each blood vessel size categories 1 to 5; note also the cross-sectional area (μm^2) represented by each size category. *Columns,* median; *bars,* upper and lower limits of the interquartile range: the lower limit is the 25th percentile and the upper limit is the 75th percentile. Fifty percent of the data lie in the interquartile range, which is a stable measure of dispersion for small samples. A tabular presentation in which these data are expressed as means $\pm$ SEM or medians with 95% confidence intervals can be accessed at http://cpl.colostate.edu/angiogenesis. **A** and **B.** Count data are number of blood vessels per unit of assessed area (mm^2) falling within the indicated vessel size criteria. **C** and **D.** Area data are blood vessel area (μm^2) per unit of assessed area (mm^2) falling within the indicated vessel size criteria. To plot total blood vessel count data, the scale used on the *y* axis in **B** is different from that used on **A**. For the same reason, the scale used on the *y* axis of **D** to plot blood vessel area is different from that used on **C**; it also was necessary to plot the area data for vessel size category 5 on **D**. Vascular density was significantly higher in IDP or DCIS relative to TEB ($P < 0.0001$) whether data were expressed as blood vessel counts or blood vessel area per unit area assessed. Total vascular density increased with morphologic progression (mild IDP $\rightarrow$ moderate IDP $\rightarrow$ florid IDP $\rightarrow$ DCIS). This trend in total vascularity was significant for total counts ($P = 0.03$) and total area ($P = 0.003$) based on the Jonckheere-Terpstra test for ordered alternatives. Total vascular density, count or area, was higher in AC than in IDP ($P < 0.001$). Vascular density also was higher in mammary carcinomas than in DCIS for count data ($P = 0.01$) but not area data ($P = 0.14$).

investigation of their angiogenic activity *ex vivo* (19), (3) the evaluation of the recruitment of endothelial cell precursors to a s.c. injected angiogenic EHS-RBM pellet (38), and (4) the extrapolation of the effects of agents on intratumoral microvessel density to the cancer prevention context (39).

In the majority of published studies of angiogenesis and premalignant breast disease progression, blood vessels associated with various pathologies have been counted. In comparing these studies, it is imperative to underscore that counting blood vessels permits only assessment of vascularity not angiogenesis (6, 10). Therefore, the investigation of angiogenesis based on vascular density represents inference that is dependent on the ''biological context'' in which the data are collected. If this factor is not taken into account in data interpretation, it could lead to misinformation about how agents that affect blood vessel formation and growth inhibit the carcinogenic process. As discussed below, we undertook a detailed analysis of the number, size, and location of all countable blood vessels that could be identified at various morphologically distinct stages of the carcinogenic process to address this problem. To our knowledge, such a detailed analysis of vascularity by vessel size has not been used previously in the investigation of angiogenesis and premalignant breast disease progression.

A key problem in making inferences about angiogenesis based on tissue vascularity is the inability to distinguish between native microvessels and pathology-associated neovascularization when immunostaining and vessel counting are used to quantify vascularity, a problem accentuated when factor VIII is used for immunostaining and/or the hot spot technique is used to identify regions within a tissue that are evaluated (6, 9, 10, 27). For this reason, CD31 rather than factor VIII immunostaining was used in this work because it enhances the ability to detect new microvessels. In addition, all identifiable blood vessels were counted using the hot spot approach, and digital analysis permitted measurement of the size of all vessels that were counted. As reported previously (30), we have proposed that microvessels that are <25 μm^2 in cross-sectional area (particularly those <10 μm^2) have a high probably of being newly formed; having vessel count data categorized by size improves the ability to make inferences about angiogenic activity from vascular density data. Next, we will discuss how vascularization changed during mammary carcinogenesis, what those changes imply about the investigation of angiogenesis and cancer prevention, and how our findings compare with those reported on humans and other rodent models for breast carcinogenesis.

Terminal End Buds. Because the TEB is the morphologic structure reported to be the target of carcinogenic insult in the rat mammary gland and the structure from which premalignant pathologies emerge (40), we considered it important to determine whether the vascularization of TEBs was affected by carcinogen treatment. If vascularization was increased, then a decrease in vascularity of TEB by a cancer preventive agent would be expected to inhibit the carcinogenic process and could potentially be used as an early marker of antiangiogenic

Table 3. Vascular density of mammary carcinomas and pregnant mammary gland as categorized by blood vessel size

	n	DPC	Region	Type	Vessel Size Classification Scheme (μm^2)					
					≤10	>10 and ≤25	>25 and ≤50	>50 and ≤75	>75	Total
AC	18	35	ET	Count	61.1 (28.3, 57.4)	174.8 (132.6, 285.3)	90.2 (63.9, 117.7)	35.5 (25.5, 40.5)	112.1 (99.4, 139.7)	525.9 (382.2, 583.6)
				Area	475.6 (187.8, 657.3)	2,867.8 (2,241.7, 4,652.9)	3,098.9 (2,165.4, 4,069.6)	2,154.7 (1,490.1, 2,527.6)	51,557.0 (28,348.7, 73,397.0)	60,786.9 (40,166.1, 85,536.7)
AC	18	35	IT	Count	9.1 (2.5, 18.6)	28.0 (13.9, 56.1)	11.0 (5.6, 17.9)	3.5 (0.0, 7.9)	6.8 (2.3, 11.9)	60.5 (35.1, 103.1)
				Area	59.3 (21.8, 130.3)	451.4 (207.3, 910.8)	435.0 (180.3, 648.4)	225.7 (0.0, 499.6)	1,065.3 (192.3, 1,980.9)	2,507.2 (1,548.7, 3,616.4)
AC	18	35	Total	Count	34.3 (11.9, 50.1)	92.8 (65.8, 150.9)	41.8 (34.5, 48.7)	16.6 (12.9, 20.9)	49.4 (40.2, 55.4)	228.4 (162.4, 321.9)
				Area	263.6 (83.3, 368.8)	154.4 (1,090.3, 2,437.0)	1,461.7 (1,230.6, 1,673.2)	1,025.5 (797.8, 1,287.5)	18,988.6 (12,446.8, 31,712.4)	23,485.0 (16,661.6, 37,347.7)
MPMG	8	0	EL	Count	36.9 (24.7, 56.1)	330.5 (208.4, 381.7)	84.4 (51.1, 138.1)	0.0 (0.0, 16.4)	7.23 (0.0, 28.3)	502.5 (356.8, 564.7)
				Area	270.8 (206.3, 448.0)	5,840.4 (3,728.0, 6,569.3)	3,081.3 (1,670.3, 4,450.8)	0.0 (0.0, 921.7)	1,577.0 (0.0, 6,079.7)	11,506.0 (10,376.1, 14,840.0)
MPMG	8	0	IL	Count	283.7 (203.4, 424.7)	739.6 (603.7, 853.0)	79.3 (69.3, 120.2)	24.6 (11.2, 47.9)	24.0 (0.0, 66.9)	1,222.0 (1,037.7, 1,359.0)
				Area	2,040.5 (1,546.8, 3,229.5)	11,142.4 (9,691.9, 13,325.2)	3,183.4 (2,208.2, 3,987.1)	1,406.2 (673.4, 3,105.7)	2,493.2 (0.0, 19,035.5)	28,268.6 (18,992.3, 35,295.0)
MPMG	8	0	Total	Count	162.1 (112.0, 226.7)	451.3 (407.6, 565.6)	110.0 (60.1, 123.1)	11.8 (9.5, 23.4)	13.1 (0.0, 49.6)	787.3 (656.5, 888.2)
				Area	1,218.9 (830.5, 1,713.9)	7,330.6 (6,908.7, 8,919.9)	3,501.8 (2,079.3, 4,221.3)	686.3 (541.0, 1,478.1)	1,776.5 (0.0, 13,551.7)	17,543.4 (13,865.8, 24,359.2)

NOTE: DPC, days post carcinogen. For AC, blood vessel sizes were counted in a 50 μm wide band circumscribing each carcinoma, the extratumoral region (ET), and within each carcinoma, the intratumoral region (IT). For MPMG, blood vessels were counted in a 50 μm band circumscribing each lobule (EL), and within each lobule, intralobular region (IL). All values are expressed as medians (upper limit, lower limit of the interquartile range: the lower limit is the 25th percentile and the upper limit is the 75th percentile). Fifty percent of the data lie in the interquartile range, which is a stable measure of dispersion for small samples. A tabular presentation in which these data are expressed as means ± SEM or medians with 95% confidence intervals can be accessed at http://cpl.colostate.edu/angiogenesis. Count data are number of blood vessels per unit of assessed area (mm^2) within the indicated vessel size criteria. Area data are blood vessel area (μm^2) per unit of assessed area (mm^2) within the indicated vessel size criteria. Total vascular density and vascular density in all vessel size categories were higher in mammary carcinomas than in DCIS ($P < 0.001$).

cancer preventive activity. Data in Table 2 are consistent with what is known about the biology of TEB but provide no support for carcinogen treatment associated differences in their vascularization. Specifically, the data showed that only a limited number of TEBs had blood vessels within the region circumscribed by a 50 μm wide band around each structure. This is expected given that (1) the vascular density analysis was performed on a 4 μm thick section of a three-dimensional structure, (2) we limited our analyses to a 50 μm wide band for the reasons mentioned in Materials and Methods, and (3) the limit for diffusion of nutrients and metabolic wastes to and from a capillary is 100 to 120 μm. When effects on specific vessel size categories were considered based on data in Table 2, there was evidence of a modest increase in new vessel formation between 21 and 49 or 56 days of age, an observation that is consistent with the fact that TEBs differentiate into alveolar buds during the time course of our study. However, no evidence was obtained that this effect was related to carcinogen treatment. To test rigorously the question of whether there might be carcinogen treatment associated changes in vascularization limited to TEBs that have the potential to progress to IDP, cluster analyses were performed to determine if subpopulations of TEB existed; however, no evidence of subpopulations of TEB that differed by vascularization was found. Data in Table 2 imply that TEBs are unlikely to be a target for antiangiogenic chemoprevention and that differences in the vascular density of TEBs cannot serve as a biomarker for assessing antiangiogenic cancer prevention modalities.

The lack of effect of carcinogen treatment mediated transformation of TEBs on vascular density of this structure is consistent with the works of Ottinetti and Sapino (6) and Fregene et al. (7) using human breast tissue but is contrary to what is predicted by the work of Heffelfinger et al. (10) using human breast tissue but is contrary to what is predicted by the work of Heffelfinger et al. (10) using human breast tissue or mammary tissue from rats treated with 7,12-dimethylbenz-α-anthracene (19). At least one reason for these discrepancies may be related to differences among laboratories in the approach to assessing vascularity and the resulting inferences made about angiogenesis.

Premalignant Mammary Pathologies

IDP and DCIS. The earliest premalignant pathology observed during chemically induced mammary carcinogenesis using the rat model system described in this study is the IDP (16, 40). Our first goal in the analysis of the data in Fig. 4 was to determine if TEBs differed markedly in vascularization relative to IDP. In first comparing TEB and IDP with mild hyperplasia, it was observed that total vascularization (count or area) was higher in IDP (mild) than TEB ($P = 0.012$). Inspection of the data in Fig. 4 shows that this increase was attributed to the number and area of blood vessels of size category ≥3 without appreciable differences in the number or area of blood vessels in size categories 1 and 2. Keeping in mind that TEB and IDP were examined from animals of the same age as well as the difficulty of discriminating between native and newly formed blood vessels in studies such as this, we suggest that the increase in blood vessel number and area observed is due in part to the larger size of IDP relative to TEB (the average size of TEB was 14,996 μm^2, whereas the average area of the mild IDPs evaluated was 83,057 μm^2) that brings the cells within these structures into closer proximity to existing blood vessels in the mammary gland and in part to the stimulation of new blood vessel formation (note that the number and area of blood vessels in size category 2 are similar in both TEB and mild IDP and that we infer that they are likely to represent developing new blood vessels).

The next issue that was addressed was to determine if vascularization increased during progression within IDP from mild to florid hyperplasia and to DCIS. Data in Fig. 4 show a numerical trend for total vascular density expressed as count or area to increase with increasing degree of hyperplasia and DCIS. Inspection of data in Fig. 4 revealed no significant changes in the count or area of blood vessels in size classes 1 or 2 in the transition from mild to florid hyperplasia or DCIS. Rather, the data indicate that the primary effect was in the vascular area accounted for by vessels in size categories 3 to 5. While some aspects of these findings are consistent with data from the human disease as reported by several laboratories, they differ in other respects from the same work (6-10, 19, 36). For example, Ottinetti and Sapino observed vascular dilation associated with mammary hyperplasias but did not observe an increase in vessel number. On the other hand, Heffelfinger et al. (10) concluded that there was an increase in vascularity during the progression of premalignant breast disease, but in the 7,12-dimethylbenz(*a*)anthracene-induced mammary carcinogenesis model, they concluded that IDP was the most vascular and presumably angiogenic stage of the disease process (19).

Because no significant differences were observed between TEB and IDP or DCIS in the number or area of blood vessels ≤25 μm, as observed in AC and MPMG (discussed below), our interpretation is that angiogenic activity in these pathologies does not appear to be induced to a greater extent than observed in TEB. This interpretation is consistent with the findings of other reports in humans (6, 7) and in part with those of ref. 9 but differs markedly from other reports using human tissue (10) or a rodent model (19). One factor contributing to these discrepancies is likely to be differences in methodology and the assumptions made in making inferences about angiogenesis-based tissue vascularity. Nonetheless, the implications of these discrepancies are considerable. In our view, data in Fig. 4 argue that dramatic effects of antiangiogenesis agents on the progression of transformed cells within TEB to IDP of increasing cellularity and to DCIS should not be anticipated, whereas such an effect would be predicted by the work reported in ref. 19.

Mammary Carcinomas. A defining step in carcinogenesis is the conversion of premalignant pathologies to invasive carcinomas. The changes in vascularization that accompany this conversion are shown in Fig. 4 and Table 3. There is an increase in total vascularization, measured as count or area, in mammary carcinomas relative to IDP or DCIS. However, data in Fig. 4 reveal that the reasons for this increase are different than observed in the comparison of TEB with either IDP or DCIS (i.e., the pattern of vascularization in mammary

carcinomas is shifted). Specifically, there is a marked increase in the number and area of vessels in size categories 1 and 2 with only small changes in count and area of larger vessels. We interpret these data to indicate that the rate of new blood vessel formation is dramatically elevated during the transition from premalignant to malignant stages of mammary carcinogenesis in this model system, and this finding is in agreement with similar observations in studies using human tissue. Ottinetti and Sapino (6) proposed that one reason for the marked increase in vascularity between DCIS and AC is that the sprouting of new vessels around neoplastic lesions is not manifest until the integrity of the basement membrane is disrupted.

MPMG. The final question addressed involved a determination of how the vascularization of carcinomas compared with the pattern of vascularization observed in MPMG. To our knowledge, there is no other published data with which to compare our findings; nonetheless, this question is of interest because we wanted to understand quantitatively how the angiogenic stimulus induced by carcinomas compared with the antigenic response that accompanies a physiologic process involving robust development of the mammary gland. In making this comparison, it is important to note that the development of carcinomas and the development of the mammary gland during pregnancy have important commonalities and significant differences. The most important similarity is that, in both cases, there is a marked increase in mammary epithelial cell number, which necessitates increased blood supply. However, cell number accumulation during pregnancy is diffuse, uniform, and organized and does not involve disruption in the integrity of the basement membrane, whereas, in carcinomas, the increase in cell number is focal, nonuniform, and disorganized and does involve disruption of the basement membrane. As shown in Fig. 4 and Table 3, there are marked differences in patterns of vascularization. Our initial analysis focused on the vascularization (50 μm boundary) around developing lobules or developing carcinomas. Interestingly, for total vascularity, there were three times more vessels in the pregnant gland than in the extratumoral region surrounding carcinomas; however, there was a 2-fold increase in vascular area in the extratumoral region of mammary carcinomas versus the peripheral region surrounding lobules in the MPMG. Not unexpectedly, data in Table 3 reveal that there is a dramatic increase in the number and area of vessels in size categories 1 to 3 in the MPMG versus carcinomas, whereas there were relatively few large blood vessels in MPMG compared with those observed in carcinomas. Similar patterns were observed when the vascular density in the intratumoral region of AC and the intralobular vascularization of the MPMG were compared. Thus, we interpret these data to indicate that pregnancy does induce angiogenesis and that the intensity of the signaling is markedly greater in the mammary gland during pregnancy relative to that observed in developing mammary carcinomas. The differences in patterns of vascularization seen in MPMG versus mammary carcinomas are likely to reflect the orderly program of mammary gland growth and differentiation during pregnancy, which is dismantled at the end of lactation versus the misregulated developmental plan that favors the selective expansion of developing clones of transformed cells. It is noteworthy that the distinction observed between patterns of vascularization in these two contexts provides an excellent example of the value of quantifying vascular density in terms of both area and counts as well as the advantage to data interpretation provided by dividing vessels into size categories.

Summary and Implications. Evidence has been presented that shows that, in this model system for breast cancer in which premalignant development of transformed ductal mammary epithelial cells to IDP and DCIS mirrors that observed in the human disease, premalignant disease progression is accompanied by an increased density of blood vessels, primarily $\geq 25\ \mu m^2$ in cross-sectional area. It remains to be determined whether this increase reflects a selection for the clonal expansion of cells in well-vascularized areas, the ability of premalignant mammary pathologies to induce the size expansion of existing vessels or cause dilation by influencing blood flow, or the encroachment by pathologies that are expanding in size on native blood vessels. On the other hand, Fig. 4 provides strong support for interpreting the vascular density data to imply that mammary carcinomas induced new blood vessel formation, apparently as transformed cells make a transition from florid IDP and DCIS to AC, a process that is accompanied by loss of basement membrane integrity.

These findings have important implications for the investigation of antiangiogenesis strategies for cancer prevention. Specifically, they indicate that antiangiogenic compounds should inhibit the progression of IDP and DCIS to carcinomas and slow the rate of tumor growth, although this prediction is at odds with a recently reported chemoprevention study of an antiangiogenic agent (36). Based on the data in Fig. 4 and Tables 2 and 3, we predict that an effective antiangiogenic chemopreventive agent would result in (1) an accumulation of premalignant mammary pathologies, (2) a reduction in the number of mammary carcinomas observed, and (3) a decrease in the size of the tumors that do occur. These predictions can be tested in the animal model described herein. Relative to measurements of vascular density and the production of proangiogenic factors, our findings imply that an effective antiangiogenic agent would reduce the density of blood vessels both within a carcinoma and those in the tissue immediately adjacent to the tumor. Finally, these data indicate that antiangiogenic agents would be expected to inhibit carcinogenesis when treatment is initiated throughout the disease process including late stages of premalignant development, with less impact anticipated on the progression of transformed cells in TEB to IDP of increasing cellularity or DCIS.

As indicated earlier, this is a complex area in which there are considerable differences in the evidence that morphologic progression is accompanied by new blood vessel formation. Only additional studies will resolve what appears to be a host of contradictory findings. However, as more is learned, these apparent discrepancies will actually provide unique insights about the role of blood vessel formation in the selection and expansion of clones of transformed mammary epithelial cells and how various subpopulations of cells progress to cancer.

References

1. Vainio H. Targeting angiogenesis—a novel mode in cancer chemoprevention. Asian Pac J Cancer Prev 2003;4:83-6.
2. Bisacchi D, Benelli R, Vanzetto C, Ferrari N, Tosetti F, Albini A. Anti-angiogenesis and angioprevention: mechanisms, problems and perspectives. Cancer Detect Prev 2003;27:229-38.
3. Pfeffer U, Ferrari N, Morini M, Benelli R, Noonan DM, Albini A. Antiangiogenic activity of chemopreventive drugs. Int J Biol Markers 2003;18:70-4.
4. Folkman J. Tumor angiogenesis: therapeutic implications. N Engl J Med 1971;285:1182-6.
5. Brem SS, Jensen HM, Gullino PM. Angiogenesis as a marker of preneoplastic lesions of the human breast. Cancer 1978;41:239-44.
6. Ottinetti A, Sapino A. Morphometric evaluation of microvessels surrounding hyperplastic and neoplastic mammary lesions. Breast Cancer Res Treat 1988;11:241-8.
7. Fregene TA, Kellogg CM, Pienta KJ. Microvessel quantification as a measure of angiogenic activity in benign breast tissue lesions: a marker for precancerous disease. Int J Oncol 1994;4:1199-202.
8. Guinebretiere JM, Le Monique G, Gavoille A, Bahi J, Contesso G. Angiogenesis and risk of breast cancer in women with fibrocystic disease [letter; comment]. J Natl Cancer Inst 1994;86:635-6.
9. Guidi AJ, Fischer L, Harris JR, Schnitt SJ. Microvessel density and distribution in ductal carcinoma in situ of the breast. J Natl Cancer Inst 1994;86:614-9.
10. Heffelfinger SC, Yassin R, Miller MA, Lower E. Vascularity of proliferative breast disease and carcinoma in situ correlates with histological features. Clin Cancer Res 1996;2:1873-8.
11. Heffelfinger SC, Miller MA, Yassin R, Gear R. Angiogenic growth factors in preinvasive breast disease. Clin Cancer Res 1999;2867-76.
12. Russo J, Gusterson BA, Rogers AE, Russo IH, Wellings SR, van Zwieten MJ. Comparative study of human and rat mammary tumorigenesis. Lab Invest 1990;62:244-78.
13. Wellings SR, Jensen HM. On the origin and progression of ductal carcinoma in the human breast. J Natl Cancer Inst 1973;50:1111-8.
14. Wellings SR, Jensen HM, Marcum RG. An atlas of subgross pathology of the human breast with special reference to possible precancerous lesions. J Natl Cancer Inst 1975;55:231-73.
15. Wellings SR. A hypothesis of the origin of human breast cancer from the terminal ductal lobular unit. Pathol Res Pract 1980;166:515-35.
16. Singh M, McGinley JN, Thompson HJ. A comparison of the histopathology of premalignant and malignant mammary gland lesions induced in sexually immature rats with those occurring in the human. Lab Invest 2000;80:221-31.
17. Maiorana A, Gullino PM. Acquisition of angiogenic capacity and neoplastic transformation in the rat mammary gland. Cancer Res 1978;38:4409-14.
18. Brem SS, Gullino PM, Medina D. Angiogenesis: a marker for neoplastic transformation of mammary papillary hyperplasia. Science 1977;195:880-2.
19. Heffelfinger SC, Gear RB, Taylor K, et al. DMBA-induced mammary pathologies are angiogenic in vivo and in vitro. Lab Invest 2000; 80:485-92.
20. Gimbrone MA Jr, Gullino PM. Neovascularization induced by intraocular xenografts of normal, preneoplastic, and neoplastic mouse mammary tissues. J Natl Cancer Inst 1976;56:305-18.
21. Gimbrone MA Jr, Gullino PM. Angiogenic capacity of preneoplastic lesions of the murine mammary gland as a marker of neoplastic transformation. Cancer Res 1976;36:2611-20.
22. Gullino PM. Natural history of breast cancer. Progression from hyperplasia to neoplasia as predicted by angiogenesis. Cancer 1977; 39:2697-703.
23. Gullino PM. Angiogenesis and oncogenesis. J Natl Cancer Inst 1978; 61:639-43.
24. Jensen HM, Chen I, DeVault MR, Lewis AE. Angiogenesis induced by ''normal'' human breast tissue: a probable marker for precancer. Science 1982;218:293-5.
25. Gullino PM, Pettigrew HM, Grantham FH. *N*-nitrosomethylurea as mammary gland carcinogen in rats. J Natl Cancer Inst 1975;54: 401-14.
26. Thompson HJ, McGinley JN, Rothhammer K, Singh M. Rapid induction of mammary intraductal proliferations, ductal carcinoma in situ and carcinomas by the injection of sexually immature female rats with 1-methyl-1-nitrosourea. Carcinogenesis 1995;16: 2407-11.
27. McGinley JN, Knott KK, Thompson HJ. Semi-automated method of quantifying vasculature of 1-methyl-1-nitrosourea-induced rat mammary carcinomas using immunohistochemical detection. J Histochem Cytochem 2002;50:213-22.
28. Thompson HJ, Singh M, McGinley J. Classification of premalignant and malignant lesions developing in the rat mammary gland after injection of sexually immature rats with 1-methyl-1-nitrosourea. J Mammary Gland Biol Neoplasia 2000;5:201-10.
29. Weidner N, Folkman J. Tumoral vascularity as a prognostic factor in cancer. Important Adv Oncol 1996;167-90.
30. Thompson HJ, McGinley JN, Knott KK, Spoelstra NS, Wolfe P. Vascular density profile of rat mammary carcinomas induced by 1-methyl-1-nitrosourea: implications for the investigation of angiogenesis. Carcinogenesis 2002;23:847-54.
31. Long JS, Freese J. Redicted probabilities for count models. STATA J 2001;1:51-7.
32. Tobin J. Estimation of relationships for limited dependent variables. Econometrica 1958;26:24-36.
33. Westfall PH, Young SS. Resampling-based multiple testing. New York: John Wiley & Sons; 1993.
34. Hollander M, Wolfe DA. Nonparametric statistical methods. New York: John Wiley & Sons; 1999.
35. Thompson HJ, McGinley JN, Wolfe P, Singh M, Steele VE, Kelloff GJ. Temporal sequence of mammary intraductal proliferations, ductal carcinomas in situ and adenocarcinomas induced by 1-methyl-1-nitrosourea in rats. Carcinogenesis 1998;19:2181-5.
36. Heffelfinger SC, Gear RB, Schneider J, et al. TNP-470 inhibits 7,12-dimethylbenz[*a*]anthracene-induced mammary tumor formation when administered before the formation of carcinoma in situ but is not additive with tamoxifen. Lab Invest 2003;83: 1001-11.
37. Singh RP, Sharma G, Dhanalakshmi S, Agarwal C, Agarwal R. Suppression of advanced human prostate tumor growth in athymic mice by silibinin feeding is associated with reduced cell proliferation, increased apoptosis, and inhibition of angiogenesis. Cancer Epidemiol Biomarkers & Prev 2003;12:933-9.
38. Masso-Welch PA, Zangani D, Ip C, et al. Inhibition of angiogenesis by the cancer chemopreventive agent conjugated linoleic acid. Cancer Res 2002;62:4383-9.
39. Jiang C, Jiang W, Ip C, Ganther H, Lu J. Selenium-induced inhibition of angiogenesis in mammary cancer at chemopreventive levels of intake. Mol Carcinog 1999;26:213-25.
40. Russo J, Russo IH. Boundaries in mammary carcinogenesis. Basic Life Sci 1991;57:43-57.

Targeting Angiogenesis for Mammary Cancer Prevention: Factors to Consider in Experimental Design and Analysis

Henry J. Thompson, John N. McGinley, Pamela Wolfe, et al.

Cancer Epidemiol Biomarkers Prev 2004;13:1173-1184.